A Fourier Analysis of Digital Beamforming with Severely Quantized mmWave Arrays

Canan Cebeci and Upamanyu Madhow
ECE Dept., University of California, Santa Barbara
Email: {ccebeci, madhow}@ucsb.edu

***Abstract*—Recent progress in silicon radio frequency integrated circuits (RFICs) has opened the possibility of fully digital massive MIMO with hundreds of antennas in millimeter wave (mmWave) bands. A critical bottleneck in "mostly digital" processing is the cost and power consumption of analog-to-digital converters (ADCs). We consider here a mmWave massive MIMO receiver employing 1-bit ADCs, a particularly energy-efficient choice, in a regime where prior work on Bussgang linearization does not apply: a small number of users propagating over spatially sparse mmWave channels. We investigate beamspace techniques based on a spatial FFT across antenna elements, which concentrates the energy of each user to a small number of FFT bins. We provide a Fourier analysis of the spatial harmonics for one user through one path, characterizing the impact of the ADC nonlinearity, along with the aliasing and spectral spread due to sampling and windowing corresponding to an array with a finite, discrete number of antennas. The analysis provides guidance on training sequence design for isolating the "fundamental" spatial frequency corresponding to the true angle of arrival. Simulations show that the design succeeds in suppressing higher-order harmonics for two users with disparate power levels.**

***Index Terms*—All-digital massive MIMO, mmWave, 1-bit ADC**

I. Introduction

With advances in CMOS radio frequency integrated circuits (RFICs), massive mmWave MIMO systems with fully digital beamforming are within reach. A significant bottleneck, however, is the energy consumption and cost of ADCs. Reducing the ADC precision down to 1 bit is an appealing design choice in this regard, and prior work based on Bussgang linearization shows that, when the input to each antenna can be modeled as approximately Gaussian, acceptable performance can be obtained due to the averaging of quantization noise over a large number of antennas. In this paper, we investigate the performance of 1-bit quantized massive MIMO in an unfavorable setting in which the number of users is small (so the input is not well-modeled as Gaussian) and the signal-to-noise ratio (SNR) is high (so noise dithering does not "soften" the impact of quantization). Such a situation could arise, for example, in small picocells, where a base station might be serving a small number of users moving too rapidly for effective power control.

A. Contributions

We begin (in Section II) with a Fourier analysis of the spatial harmonics for the noiseless received signal for a single user, accounting for the ADC nonlinearity, and the sampling and windowing associated with a finite, discrete array. We numerically illustrate how the relative strengths of the harmonics depend on the SNR per receive element. In Section III, we provide a link budget analysis for a mmWave MIMO uplink at 140 GHz showing that nonlinear effects related to a "too high" SNR can indeed appear at reasonably large link distances. Specializing then to the high SNR setting, we observe in Section IV that standard training sequences are unable to separate the fundamental spatial harmonic of interest from higher order spatial harmonics. We employ our Fourier analysis to develop guidelines on training sequence design for isolating the fundamental spatial frequency. Simulation results show that this design approach is effective for two users even with large power disparities.

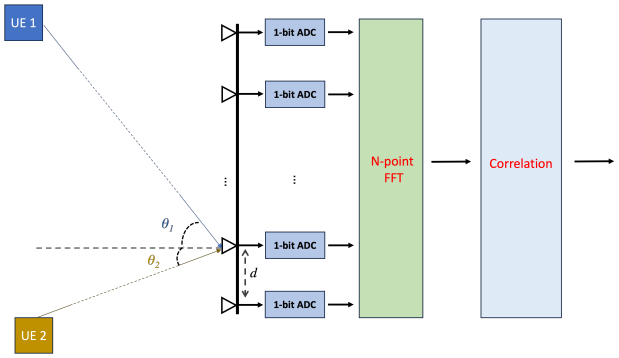

Fig. 1: A severely quantized massive MIMO uplink with beamspace processing and time domain correlation with an appropriately designed training sequence.

B. Related Work

For a regularly spaced array, the array response corresponding to the dominant path for a given user is a complex exponential, so that taking a spatial FFT across antenna elements concentrates the user energy into a small number of bins: such a transformation into "beamspace" [1] vastly simplifies operations such as multiuser detection, channel estimation, and transmit precoding, and limiting computational complexity as we scale up the number of elements. Prior work on the impact of reduced ADC precision for all-digital massive multiuser MIMO [2], [3] utilizes the Bussgang decomposition, modeling the input to each antenna as approximately Gaussian, and shows that quantization noise can be effectively averaged over a large number of antennas. While mmWave channels are sparse (e.g., each user's spatial channel may be dominated by a

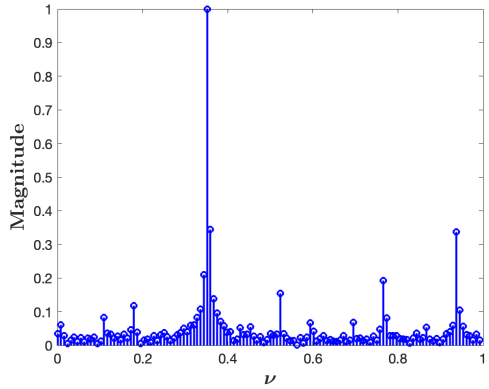

(a)

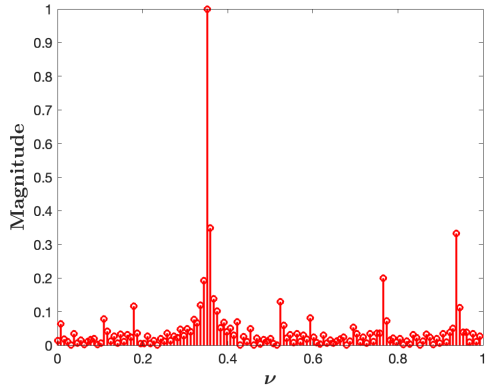

(b)

Fig. 2: (a) Normalized magnitude of the $N = 128$-point FFT of the quantized received vector for one user with $\nu = 0.3536$ without noise (b) Result of the analysis for the same case.

single path), the Gaussian approximation is still quite accurate for a moderately large number of simultaneous users [2]. Other relevant work on quantized mmWave massive MIMO includes [4]–[6]. We seek to determine the limits of beamspace processing in severely quantized mmWave MIMO systems in which the linearized regimes considered in such prior work do not apply.

Our model is reminiscent of classical analog models of sinusoids through passband hardlimiters [7]–[10], but differs in several important aspects. These classical models considers real-valued time domain sinusoids and a bandpass filter after the hardlimiter which eliminates the bulk of the harmonics and intermodulation terms. In contrast, our digital model considers complex spatial exponentials, and must incorporate the impact of sampling (so that harmonics alias back in) and windowing (leading to spectral spread).

II. Model and Analysis

Consider an N-element uplink receiver as in Fig. 1. Denoting the angle of arrival for the kth user by θ_k, the corresponding array response is a complex exponential at spatial frequency $\Omega_k = \frac{2\pi d \sin\theta_k}{\lambda}$, where d denotes the inter-element spacing (we use the standard spacing $d = \lambda/2$ in our numerical results):

$$\boldsymbol{a}(\Omega) = [e^{j0}\ e^{j\Omega}\ e^{j2\Omega} \cdots e^{j(N-1)\Omega}]^\top. \tag{1}$$

Assuming a symbol-synchronous system for simplicity, the spatial signal at the mth sample for the kth user is given by

$$\boldsymbol{s}_k[m] = A_k e^{j\phi_k} b_k[m]\boldsymbol{a}(\Omega_k) + \boldsymbol{n}[m] \tag{2}$$

where $b_k[m]$ is the mth symbol for user k, $\mathbf{n}[m] \sim \mathcal{CN}(0,\ 2\sigma^2\mathbf{I})$ is the noise vector, and A_k, ϕ_k are the channel gains and phase, respectively. Upon reception, both quadrature and in-phase parts of this antenna input undergo 1-bit quantization operation defined by $Q(a) = 1$ if $a \geq 0$, and $Q(a) = -1$ otherwise, where $a \in \mathbb{R}$. The output of the 1-bit quantization is given by

$$\boldsymbol{q}[m] = Q(\Re(\boldsymbol{s}_k[m])) + jQ(\Im(\boldsymbol{s}_k[m])). \tag{3}$$

The beamspace representation of $\boldsymbol{q}[m]$ is obtained by taking the $N-$point FFT of it:

$$\boldsymbol{y}[m] = \mathbf{FFT}(\boldsymbol{q}[m]). \tag{4}$$

We ask whether we can isolate the right FFT bins after beamspace processing for each user. We provide insight by analyzing a single-user system, and then provide simulations for two users.

A. Single user

Consider the signal $s_\Omega(x) = e^{j\Omega x}$, where x is a continuous spatial variable measured in units of $\lambda/2$, and where $\Omega \in [0, 2\pi)$ is the spatial frequency per unit length (we also define $\nu = \frac{\Omega}{2\pi} \in [0, 1)$ as the spatial frequency in cycles per unit length). The N-element array samples this signal at spacing $L = 1$ over the window $[0, N-1]$, followed by 1-bit quantization of the real and imaginary parts. Key to our analysis is the observation that we may interchange the order of these operations, first quantizing $s_\Omega(x)$, and then windowing and sampling. Adapting standard Fourier series analysis of a hardlimited sinusoid (which tells us that only the odd harmonics exist) to a setting in which the real and imaginary parts of the complex exponential are being individually hardlimited, we show that the output of the hardlimiter is complex exponentials at $(-1)^n(2n+1)\Omega_k$, $n = 0, 1, ...$ (i.e., harmonics at $+\Omega_k$, $-3\Omega_k$, $+5\Omega_k$, ...). Sampling and windowing by the antenna array create aliasing and spatial spreading of these harmonics. To illustrate the Fourier analysis matches the quantized single user input in the beamspace domain, we plot them side by side (Fig. 2).

While noise has been ignored in the preceding analysis, Fig. 3 shows how SNR impacts the output of the spatial FFT. At low SNR per element (e.g., 0 dB and below), only the fundamental spatial harmonic appears, while at 10 dB SNR per element, we clearly see both the first and third harmonics.

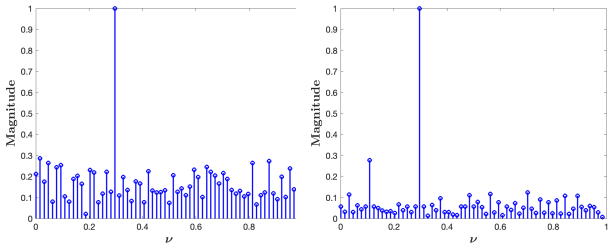

(a) SNR per antenna: 0 dB (b) SNR per antenna: 10 dB

Fig. 3: Normalized magnitude versus spatial frequency of 64-point FFT outputs. $N = 64$ and $\nu = 0.3$ for each case.

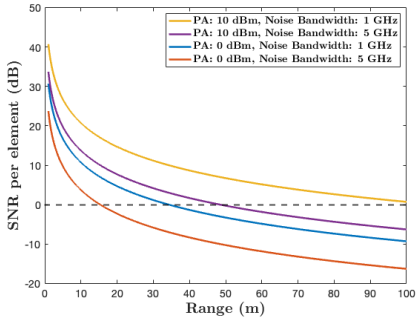

Fig. 4: Range versus SNR per element at the receiver for the given parameters.

B. Two Users

The antenna input when there are two simultaneous users communicating with the base station is given by

$$\boldsymbol{r}[m] = \sum_{k=1}^{2} (A_k e^{j\phi_k} b_k[m] \boldsymbol{a}(\Omega_k)) + \mathbf{n}[m], \tag{5}$$

where $\boldsymbol{n}[m]$ is the complex AWGN noise vector. The input goes through 1-bit quantization and FFT operations as given in Eq. 3 and 4. A Fourier analysis for two users yields far more complicated expressions than for one user; we therefore only provide simulation results here.

III. Where Does the Nonlinear Regime Start?

In this section, we carry out a link budget analysis for a mmWave MIMO uplink showing that the SNR per element can indeed be high enough to lead to nonlinear effects at moderately large link ranges. Thus, nonlinear effects must either be taken into account in the transceiver design, or appropriate power control must be exerted to ensure that SNR per element is low enough to dither the impact of the severe quantization. Consider an N-element massive MIMO uplink with line-of-sight channels. We assume the transmitter antennas are equipped with CMOS power amplifiers (with output powers in the range of 0 to 10 dBm), and that there is only free-space path loss. We determine the per-antenna SNR at the receiver as a function of range, and plot it in Fig. 4, using the following link parameters:

- number of transmit antenna elements is 16, and the transmit array is able to form an ideal beam towards the receiver,
- the gain of each individual transmit and receive elements is 2 dBi (consistent with patch elements),
- the carrier frequency is 140 GHz,
- the receiver noise figure is 6 dB,
- thermal noise is calculated for 1 and 5 GHz noise bandwidth,
- values considered for transmit power of each Power Amplifier (PA) are 0 and 10 dBm.

We see from Fig. 4 that, without power control, the high SNR per receive element (above 0 dB) regime, where we do not get the benefit of noise dithering, can occur at moderately large ranges. For example, with 10 dBm PA and noise bandwidth 5 GHz, the high SNR regime starts at around 49 m. Decreasing the noise bandwidth to 1 GHz with the same PA power, we see high SNR regimes beyond 100 m.

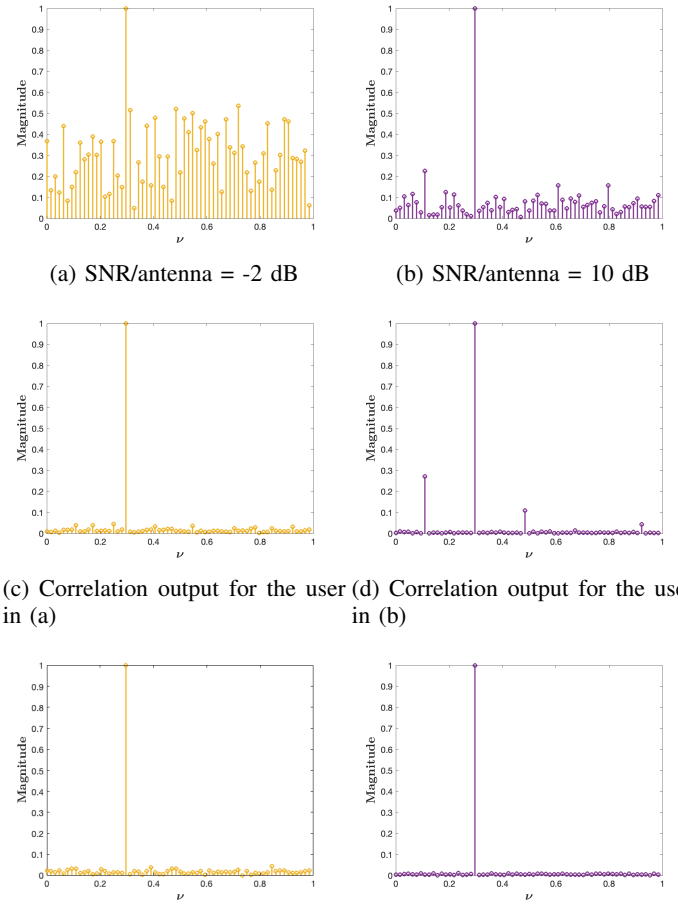

(a) SNR/antenna = -2 dB (b) SNR/antenna = 10 dB

(c) Correlation output for the user in (a) (d) Correlation output for the user in (b)

(e) Correlation output for the user in (a) (f) Correlation output for the user in (b)

Fig. 5: (a), (b) Normalized magnitudes of the 64-point FFT of a single user with QPSK signaling and $\nu = 0.3$. (c), (d) The output after correlation with a traditional training sequence. (e), (f) The output after correlation with a ramped-phase training sequence. $N_t = 100$ for (c) - (f).

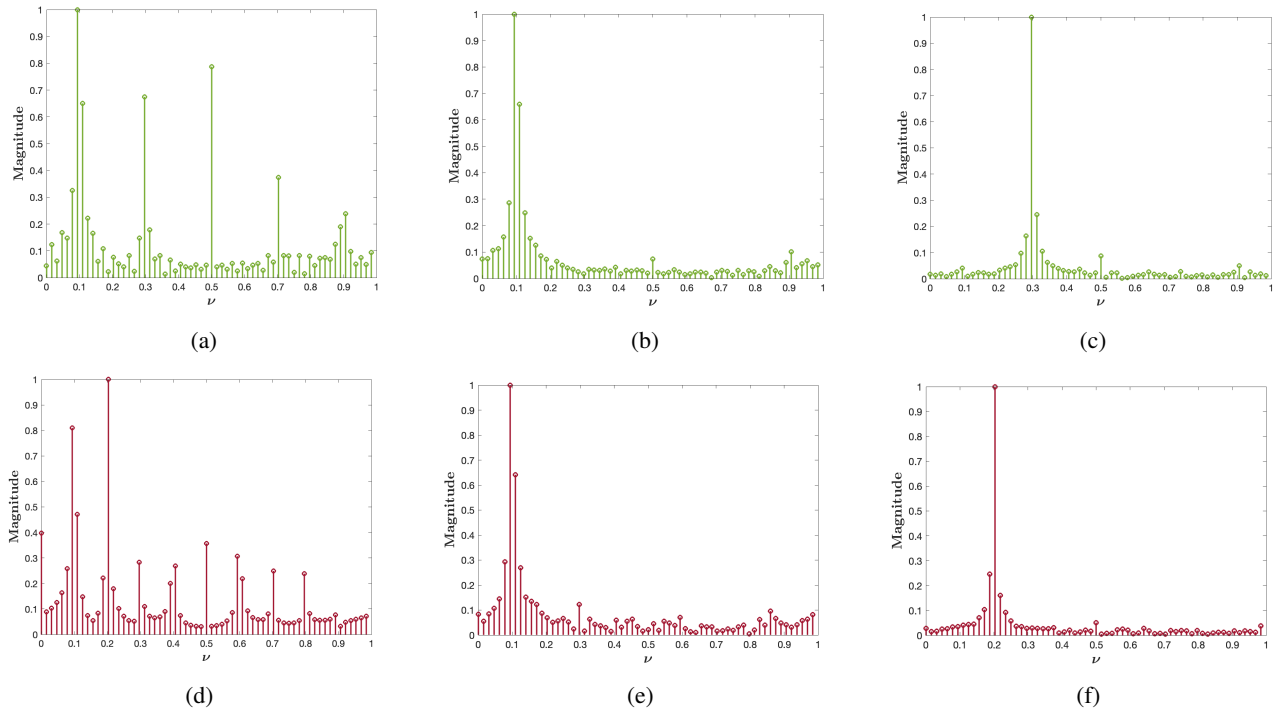

Fig. 6: (a), (d) Normalized magnitude of the N = 64-point FFT of the quantized received vector for two users, in (a) $\nu_1 = 0.1$ and $\nu_2 = 0.3$ (the harmonic mixture that occurs at $\nu = 0.5$ is larger in magnitude than the magnitude at $\nu_2 = 0.3$) with 10 dB SNR/antenna for each user, whereas in (d) $\nu_1 = 0.1$ and $\nu_2 = 0.2$ with 1 dB and 5 dB SNR/antenna for the first and second user, respectively. (b), (e) Correlation output ($N_t = 50$) for the first user. (c), (f) Correlation output ($N_t = 50$) for the second user.

IV. Training for Harmonic Suppression

The analysis provides important guidelines on training sequence design for suppressing higher-order harmonics in the high SNR regime. Denoting the length of the training sequence by N_t, the correlator output for a user is given by

$$\boldsymbol{z} = \sum_{m=1}^{N_t} \boldsymbol{y}[m] b_k^*[m]. \tag{6}$$

The Fourier analysis for 1-bit quantized complex exponential has shown that the odd harmonics of the fundamental spatial frequency will be present in the beamspace domain. Correlating the $(2n+1)$th harmonic against the phase $\phi[m]$ for the mth symbol yields

$$e^{j((2n+1)\phi[m](-1)^n)} e^{-j\phi[m]} = \begin{cases} e^{j2n\phi[m]}, & \text{if } n \text{ is even} \\ e^{j(-2(n+1))\phi[m]}, & \text{if } n \text{ is odd} \end{cases} \tag{7}$$

This shows, for example, that for single-carrier QPSK signaling, where $\phi[m] \in \{\frac{\pi}{4}, \frac{3\pi}{4}, \frac{5\pi}{4}, \frac{7\pi}{4}\}$, correlating against a training sequence is of no help in suppressing harmonics. However, if we introduce an additional phase ramp into the training sequence (e.g., $\phi[m] = m\frac{\pi}{N_t} + \psi[m]$, where $\psi[m]$ is the phase due to QPSK modulation), we can ensure that the phasors at the correlator output corresponding to higher-order harmonics sum to zero over a designated number of samples. While adding a ramped phase to the training sequence is helpful in suppressing the higher-order harmonics in the high SNR regime, a traditional training sequence works well enough in suppressing the higher-order harmonics in the low SNR regime (Fig. 5).

Fig. 6 shows simulation results for two users. We consider two scenarios: a case where one of the harmonic mixtures has a larger magnitude than one of the fundamental spatial frequencies, and a case where the power difference between the users is high. The rich harmonic structure in beamspace is shown in Fig. 6(a) and (d), while Fig. 6(b), (c), (e) and (f) show that correlation with independent QPSK training sequences, each with a phase ramp, is successful in suppressing higher-order harmonics and inter-user interference.

The distinction between low and high SNR regimes manifests itself in constellation diagrams as well. While it is expected that constellation clusters will have more spread with low SNR values, if the SNR is increased, a modulation scheme that depends on both the amplitude and phase of the symbols will exhibit merging between constellation clusters. Fig. 7 shows the constellation points for a received signal of a user with $\nu = 0.3$ with different modulation schemes. For 16QAM modulation, starting from 12 dB SNR per antenna element, we see that 16 constellation points reduce to 12 points due to loss of amplitude information in high SNR. The constellation points are obtained by a matched filter after the fundamental spatial frequency is estimated by picking the DFT bin that has the most energy, which is denoted by $\text{index}_{\text{max}}$. The estimated

channel phase ($\hat{\phi}_{\text{channel}}$) is found by

$$\hat{\phi}_{\text{channel}} = \angle \boldsymbol{z}[\text{index}_{\text{max}}]. \tag{8}$$

Denoting the estimated fundamental spatial by $\hat{\Omega}$, the matched filter output $\boldsymbol{p}[m]$ is

$$\boldsymbol{p}[m] = (e^{j\hat{\phi}_{\text{channel}}}\boldsymbol{a}(\hat{\Omega}))^{\text{H}}\boldsymbol{q}[m]. \tag{9}$$

V. Conclusion

While severely quantized massive MIMO can be understood, and designed to work well, in regimes amenable to Bussgang linearization, our work here points out the difficulties that could arise in truly nonlinear regimes with a small number of users at an excessively high SNR over spatially sparse channels. While the preferred approach is to avoid such settings (e.g., with power control), this may not always be possible. Our Fourier analysis sheds fundamental light on such regimes, providing guidance on training strategies and beamspace processing that can support large constellations despite the proliferation of higher-order spatial harmonics.

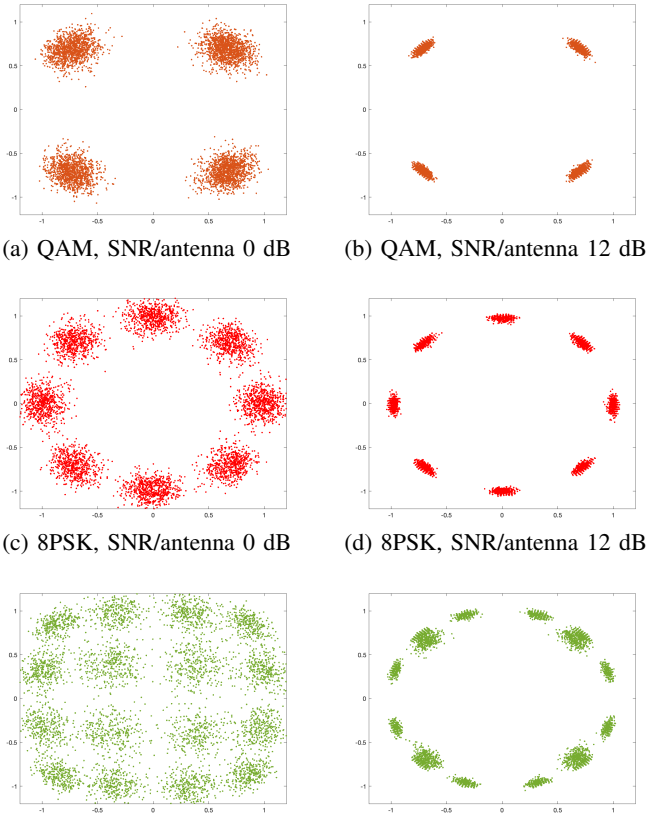

(a) QAM, SNR/antenna 0 dB (b) QAM, SNR/antenna 12 dB

(c) 8PSK, SNR/antenna 0 dB (d) 8PSK, SNR/antenna 12 dB

(e) 16QAM, SNR/antenna 0 dB (f) 16QAM, SNR/antenna 12 dB

Fig. 7: Constellation points before phase correction for different modulation schemes and SNR per antenna values. $N = 64$ for all cases.

Acknowledgment

This work was supported in part by the National Science Foundation under grant CNS-2148303 under the RINGS program, and by the Center for Ubiquitous Connectivity (CUbiC), sponsored by Semiconductor Research Corporation (SRC) and Defense Advanced Research Projects Agency (DARPA) under the JUMP 2.0 program.

References

[1] M. Abdelghany, U. Madhow, and A. Tölli, "Beamspace local LMMSE: An efficient digital backend for mmwave massive MIMO," in *2019 IEEE 20th International Workshop on Signal Processing Advances in Wireless Communications (SPAWC 2019)*.

[2] M. Abdelghany, A. A. Farid, M. E. Rasekh, U. Madhow, and M. J. W. Rodwell, "A design framework for all-digital mmwave massive MIMO with per-antenna nonlinearities," *IEEE Trans. Wireless Communications*, vol. 20, no. 9, pp. 5689–5701, 2021.

[3] L. V. Nguyen and D. H. Nguyen, "Linear receivers for massive MIMO systems with one-bit ADCs," *arXiv preprint arXiv:1907.06664*, 2019.

[4] J. Zhang, L. Dai, X. Li, Y. Liu, and L. Hanzo, "On low-resolution adcs in practical 5g millimeter-wave massive mimo systems," *IEEE Communications Magazine*, vol. 56, no. 7, pp. 205–211, 2018.

[5] J. Singh, O. Dabeer, and U. Madhow, "On the limits of communication with low-precision analog-to-digital conversion at the receiver," *IEEE Transactions on Communications*, vol. 57, no. 12, pp. 3629–3639, 2009.

[6] J. Zhang, L. Dai, S. Sun, and Z. Wang, "On the spectral efficiency of massive mimo systems with low-resolution adcs," *IEEE Communications Letters*, vol. 20, no. 5, pp. 842–845, 2016.

[7] W. Sollfrey, "Hard limiting of three and four sinusoidal signals," *IEEE Transactions on Information Theory*, vol. 15, no. 1, pp. 2–7, 1969.

[8] P. Jain, "Limiting of signals in random noise," *IEEE Transactions on Information Theory*, vol. 18, no. 3, pp. 332–340, 1972.

[9] P. Shaft, "Limiting of several signals and its effect on communication system performance," *IEEE Transactions on Communication Technology*, vol. 13, no. 4, pp. 504–512, 1965.

[10] N. Blachman, "The intermodulation and distortion due to quantization of sinusoids," *IEEE transactions on acoustics, speech, and signal processing*, vol. 33, no. 6, pp. 1417–1426, 1985.